Joint Pathology Center
Veterinary Pathology Services

WEDNESDAY SLIDE CONFERENCE 2024-2025

Conference #11 30 October 2024

CASE I:

Signalment:
A 4 year old intact Male Beagle dog (*Canis familiaris*).

History:
Presented for a 9 day history of hyporexia and regurgitation. Previous history of being treated for hepatozoonosis in April 2023 with relapse in May 2023. Radiographs revealed bilateral femoral periosteal bone reaction. Abdominal ultrasound found free fluid (which was frank blood determined via abdominocentesis) and multiple cavitated lesions in spleen and liver. An abdominal exploratory laparotomy was performed which found a ruptured splenic mass as well as two additional masses within the liver. Humane euthanasia was elected given uncertain prognosis and the remains were submitted for necropsy.

Gross Pathology:
Arising from the base of the heart immediately adjacent to the aorta are two ovoid, green to dark brown, smooth and firm nodules measuring 2 cm x 1 cm x 1 cm.

Within the abdominal cavity is approximately 32 mL of red, opaque, watery fluid. All lymph nodes are mildly to moderately enlarged, reaching up to 2 cm diameter with the abdominal lymph nodes most severely affected.

Figure 1-1. Heart, dog. Multiple sections of heart and lymph node are submitted for examination. (HE, 5X)

Laboratory Results:
Hepatozoon spp. RealPCR: Negative

Microscopic Description:
Heart: Examined are four sections. Multifocally infiltrating between and separating cardiomyocyte fibers are discrete, occasionally encapsulated, aggregates of predominantly lymphocytes and plasma cells with scattered macrophages and fibroblasts. Within several of these aggregates are reactive histiocytes containing spherical eosinophilic and intracytoplasmic round protozoan merozoites approximately 4-6µm in diameter and often displacing the host cell nuclei. Randomly distributed throughout the right, left, and interventricular septal walls are variably- sized multilamellar mucopolysaccharide rich cysts (Onion skin cysts, meronts) up to 200 µm in diameter. Occasionally within these maturing meronts are variable stages of merozoite development containing greater than 50, 2-3µm

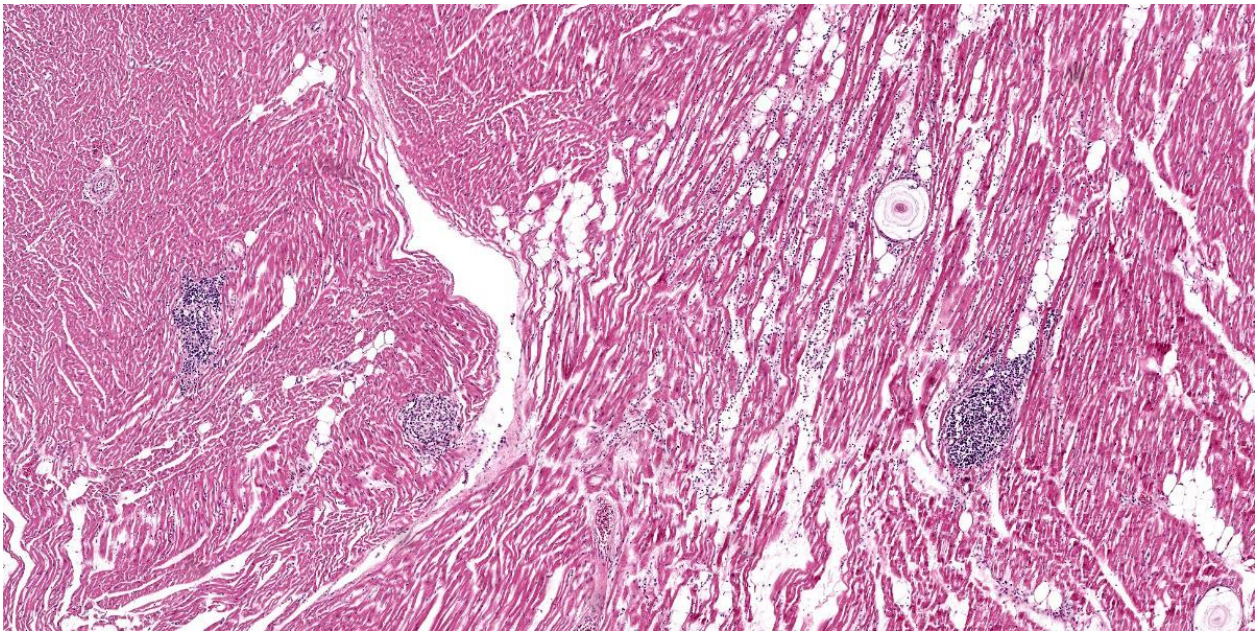

Figure 1-2. Heart, dog. There are multiple foci of hypercellularity within the myocardium as well as a single "onion-skin" cyst of *Hepatozoon americanum*. (HE, 47X)

in diameter merozoites. These meronts frequently enmesh neighboring fibrocytes and are often surrounded by rings of leukocytes. Lymphocytes and plasma cells infiltrate between the adjacent

Contributor's Morphologic Diagnosis:
Whole Body (Spleen, Lymph nodes, Heart, Blood vessels, Skeletal muscle): Chronic, multifocal lymphoplasmacytic and histiocytic inflammation with intralesional encysted protozoa (consistent with *Hepatozoon* sp.)

Contributor's Comment:
The patient's reported progressive decline was considered multifactorial, likely owing to a combination of systemic hepatozoonosis and ruptured splenic hemangiosarcoma (not captured in the provided slide). The patient's hemoabdomen noted during the abdominal exploration surgery was subsequent to the ruptured splenic hemangiosarcoma as well as several ruptured hematomas along the hepatic parenchyma. These hepatic hematomas are presumed sequela to robust, hepatozoonosis-mediated hepatitis and hepatic necrosis with pronounced hepatic parenchymal loss.

Hepatozoon is a protozoan classified among the apicomplexan phylum, primarily affecting the canine species (intermediate host) in the southeastern and central United States with several species variants noted in Latin America, Africa, Asia, and Europe.[1-9] Two primary species reported to infect domestic canids include *Hepatozoon americanum* and *Hepatozoon canis* while in felids *Hepatozoon felis*, *Hepatozoon silvestris*, and *Hepatozoon canis* are the primary species.[1] Hepatozoonosis has additionally been documented in rodent, racoon, kiwis, opossums, and wild canids.[1] Transmission of *Hepatozoon* spp. is via ingestion of arthropod vectors (direct host) with several tick species (e.g. *Rhipicephalus, Amblyomma*, and *Ixodes* spp.) being well-documented.[1-9] These ticks harbor the oocyst stage and upon ingestion release sporozoites into the host blood stream with subsequent deposition and infiltration in the spleen, bone marrow, lymph nodes, and ma

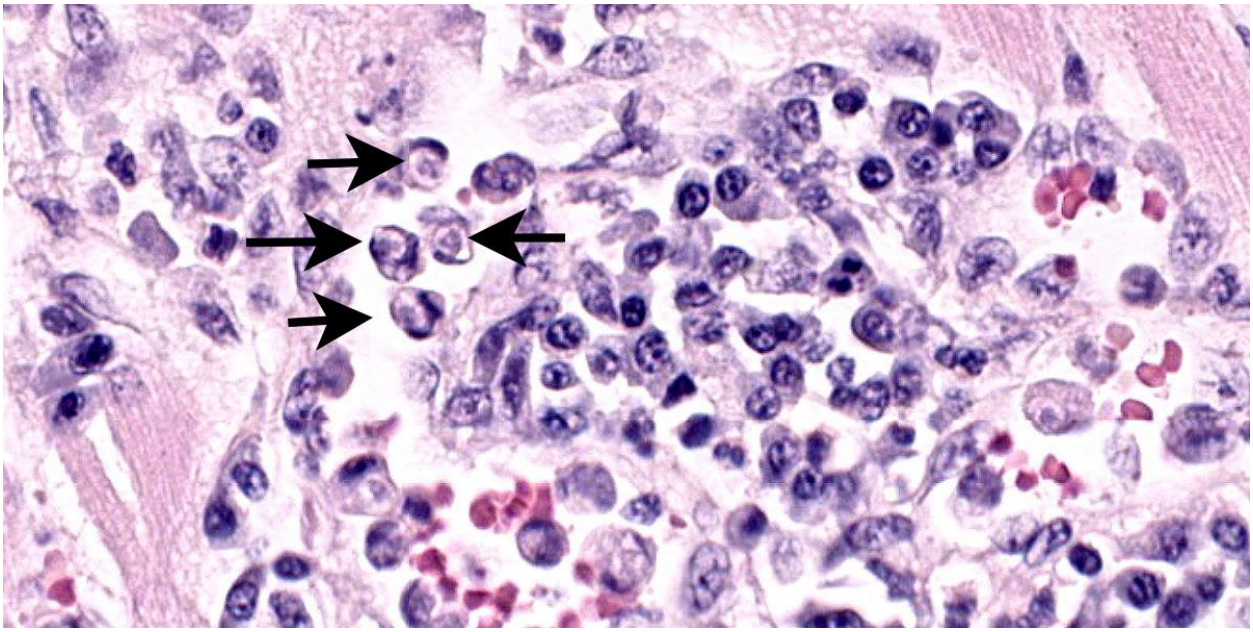

Figure 1-3. Heart, dog. Foci of hypercellularity contain moderate numbers of lymphocyte, plasma cells, and histiocytes. Within the cytoplasm of several histiocytes, there is a single protozoal meront (arrows). (HE, 1024X)

jor viscera where they encyst and form meronts.[1-9] Merozoites begin to safely develop in these seemingly innocuous meronts and are released in mass upon complete maturation, thus inciting an aggressive (typically pyogranulomatous) host response.[3] The true genius of this organism shines through, as these young merozoites safely hijack the recruited macrophages and neutrophils, escape the granuloma, and begin to undergo their final maturation into gamonts. Fully developed gamonts once again exit the leukocyte and reenter host blood circulation to be once again consumed by another tick during a hematogenous meal and perpetuate its life cycle.[1-9]

The typical gross presentation is primarily restricted to skeletal and cardiac muscle manifesting as a nonspecific myositis and muscle wasting (as evidenced in this case) but can additionally involve major organs such as bone marrow, liver, lungs, and the kidneys. A striking but less frequently observed gross finding is periosteal proliferation of the long bones, which was not observed in this case.[2,5]

On microscopic examination, the diagnostic lesion is multiple encysted approximately 250µm in diameter meronts[2] containing merozoites at varying stages of development enmeshed in a multilayered mucopolysaccharide and fibroblast-rich capsule (onion-skin cyst).[3] In systemic infection, leukocytes (macrophage, neutrophil, and monocytes) can be observed with intracytoplasmic merozoites approximately 4-6µm in diameter often displacing the host nuclei.[1,3,4] On cytologic smear intracytoplasmic gamonts can be rarely observed in monocytes.[1]

This case is an important reminder of the limitations of PCR as a confirmatory or definitive diagnostic tool. Despite both historic Hepatozoonosis and impressive multisystemic disease, the antemortem real time PCR was negative at the time of submission. A false negative PCR indicates that Hepatozoon DNA was not detected in the specific sample submission or may suggest that the numbers of detectable organisms is below the limit of

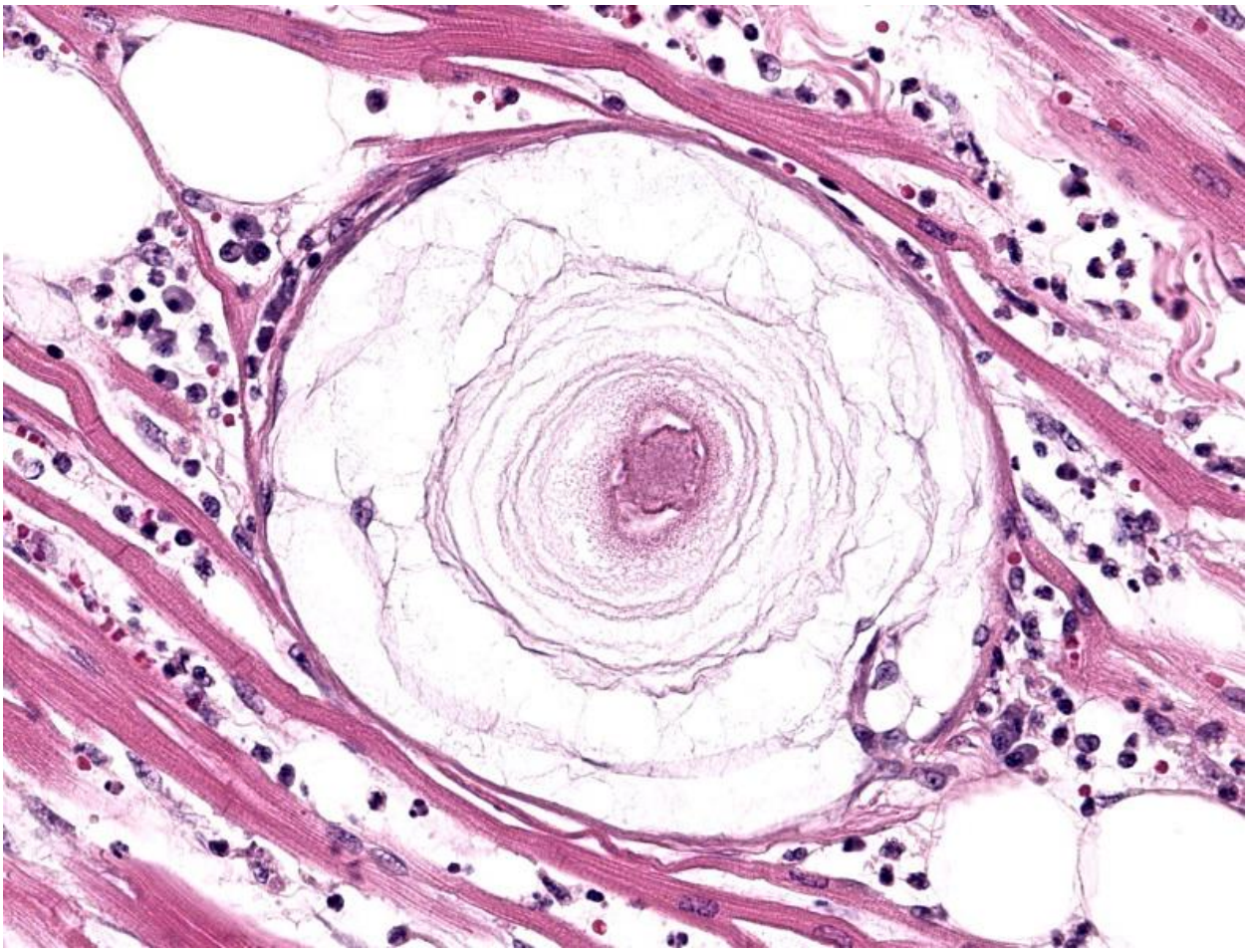

Figure 1-4. Heart, dog. High magnification of characteristic "onion-skin" cyst with multiple lamellations of mucopolysaccharide with a central host cell nucleus. There are low numbers of lymphocytes, histiocytes, and plasma cells within the interstitium. (HE, 381X)

detection (i.e. decreased numbers of organisms following treatment, a chronic carrier state, or the occurrence of new strain variations). When possible, PCR should be utilized in conjunction with corroborating tests such as cytologic blood smears, fine needle aspirates of hematopoietic and lymphoid tissue, and indirect fluorescent antibody (IFA). Muscle biopsy and/or necropsy remain the gold standard for definitive diagnosis.[1]

Contributing Institution:
North Carolina State University College of Veterinary Medicine

https://cvm.ncsu.edu/php/

JPC Diagnosis:

1. Heart: Myocarditis, histiocytic and lymphoplasmacytic, multifocal, moderate with intracellular apicomplexan meronts.
2. Lymph node: Sinus histiocytosis, diffuse, mild with apicomplexan meronts.

JPC Comment:
This week's moderator was Dr. Tony Alves, former JPC Veterinary Pathology Director and current pathologist at the National Institute of Allergy and Infectious Diseases (NIH/NIAID). Given his role within the NIAID Infectious Disease Pathogenesis Section, the theme for this conference was hardly surprising for participants.

This first case was relatively straightforward for residents (who, as WSC tradition provides, were not provided case history). From subgross magnification,, the large meronts (apicomplexan cysts) and inflammatory foci are scattered among the multiple tissues provided, underscoring that these changes contributed to the decline of this animal. The size and lamellation of these meronts along with the concurrent inflammation and hypertrophic osteopathy are highly suggestive of *H. americanum* over *H. canis*.[1,2] In the latter case, meronts are smaller and rarely incite significant inflammation. Conference participants discussed the cell of origin infected by sporozoites on the slide and concluded that cardiac myocytes and histiocytes (particularly within the lymph node) were most likely in this case. Stains for PAS, PAS-Alcian Blue, and Giemsa all reliably stained the cyst wall, mucinous material, and/or merozoites for this case.

Dr. Alves noted several ancillary features in this case, which might be overlooked at first glance, that hint at a wider clinical story.. Within the heart, there is a solitary arteriole with amorphous eosinophilic material that expands the tunica media and compresses the lumen, consistent with either hyalinosis (an aging change) or amyloidosis given the concurrent inflammation in section. Additionally, there were few megakaryocytes present within the lymph node, suggestive of extramedullary hematopoiesis in response to anemia from hemoabdomen.

Conference participants discussed several ruleouts for tissue cysts. *Trypanosoma cruzi* and *Sarcocystis* spp. both form discrete tissue cysts. In contrast to *Hepatozoon* (particularly *H. americanum*) these cysts lack lamellation (*Sarcocystis and Trypanosoma*); size and shape is variable and may appear similar. Distribution to cardiac myocytes is common among all 3 species, though distribution to other tissues (e.g. lymph node) may be a distinguishing diagnostic feature absent IHC. Additionally, smaller tissue cysts to consider are *Toxoplasma* and *Neospora*. We recently *covered T. cruzi* in WSC 2024-2025 (Conference 3, Case 3). For another example of *H. americanum* from the WSC archives, see Case 2, Conference 18, 2015-2016.

References:

1. Baneth G, Allen K. Hepatozoonosis of Dogs and Cats. *Veterinary Clinics of North America*. 2022; 52(6):1341-1358.
2. Craig LE, Dittmer KE, Thompson KG. Bones and Joints. In: Maxie MG, ed. *Jubb, Kennedy and Palmer's Pathology of Domestic Animals*. Vol 1. 6th ed. Louis, MO: Elsevier; 2016: 94
3. Cummings CA, Panciera RJ, Kocan KM, Mathew JS, Ewing SA. Characterization of stages of Hepatozoon americanum and parasitized canine host cells. *Vet Pathol*. 2005;42(6):788-796.
4. Ewing SA, Panciera RJ. American canine hepatozoonosis. *Clinical Microbiology Reviews*. 2003; 16(4):688-97.
5. Panciera RJ, Mathew JS, Ewing SA, Cummings CA, Drost WT, Kocan AA. Skeletal Lesions of Canine Hepatozoonosis Caused by Hepatozoon americanum. *Veterinary Pathology*. 2000;37(3):225-230.
6. Parkins ND, Stokes JV, Gavron NA, Frankovich AN, Varela-Stokes, JV. Scarcity of Hepatozoon americanum in Gulf Coast tick vectors and potential for cultivating the protozoan. *Vet Parasitol*. 2020
7. Potter TM, Macintire DK. Hepatozoon americanum: an emerging disease in the south-central/southeastern United States. *Journal of Veterinary Emergency and Critical Care*. 2010; 20:70-76.
8. Valli VEO, Kiupel M, Bienzle D. Hematopoietic system. In: Maxie MG, ed. *Jubb, Kennedy, and Palmer's Pathology of Domestic Animals*. 6th ed. Vol 3. St.

Louis, MO: Elsevier; 2016:109-111.
9. Van Vleet JF, Valentine BA. Muscle and tendons. Hepatozoonosis. In Maxie MG, ed. *Jubb, Kennedy and Palmer's Pathology of Domestic Animals*. 6th ed. Vol 1. Elsevier Saunders; 2007: 240.

CASE II:

Signalment:
1.2-year-old, intact female, German shepherd canine.

History:
This dog was adopted recently from a rescue in Texas. She had a history of a persistent, productive cough that worsened over time. She presented to the UWVC Small Animal Internal Medicine Service for a possible megaesophagus work up. The owner also reported occasional hemoptysis at home and hyporexia. Computed Tomography (CT) revealed a cranial mediastinal mass. Over time, her symptoms worsened and she returned to the hospital due to increased respiratory effort. Thoracic radiographs revealed aspiration pneumonia, atelectasis and confirmed the previously diagnosed static cranial mediastinal mass, which was associated with a segmental megaesophagus and compression of the trachea and primary bronchi. An endotracheal wash performed and showed neutrophilic and eosinophilic inflammation with no bacterial growth. A fine needle aspirate was taken from the mediastinal mass and showed evidence of neutrophilic and eosinophilic inflammation with rare linear material that was suggestive of fungal hyphae. Heartworm and blastomycosis antigen testing and coccidiosis titers were all negative. This dog continued to decline and euthanasia was elected.

Gross Pathology:
A locally extensive portion of the esophagus, beginning from midway down the neck and extending to the diaphragm, is markedly thickened, nodular and firm. In this region, the wall of the esophagus is massively expanded, up to 1.5 cm, by abundant firm, tan, fibrous material interspersed with well demarcated pockets of friable reddened tissue with a green tinge (see Figure 1). This change extends beyond the wall of the esophagus to incorporate the adjacent enlarged cranial mediastinal and tracheobronchial lymph nodes, the trachea and the adjacent dorsal portions of the lungs (see Figure 2). The luminal diameter of the trachea is significantly reduced. Within the most severely affected areas, the trachea is almost completely effaced by this process and the tracheal lumen has a significantly distorted and reduced diameter. The mucosal surface of the esophagus is friable and multifocally covered by plaques of stringy friable material (fibrin). Multifocally, there are variably sized areas where the mucosal epithelium is absent (ulcer), including a locally extensive 2.5 x 2 cm region.

Figure 2-1. Esophagus, dog. Gross photograph of esophagus with epiglottis (white arrow). The esophagus is markedly thickened and firm and there are locally extensive regions of ulceration. (*Photo courtesy of:* University of Wisconsin School of Veterinary Medicine, Department of Pathobiological Sciences, https://www.vetmed.wisc.edu/departments/pathobiological-sciences/)

Laboratory Results:
A panfungal PCR with sequencing identified *Cladosporium* species.

Figure 2-2. Esophagus, dog. Gross photograph of esophagus with trachea (white arrow). The process occurring in the esophagus extends to completely encapsulate the trachea, significantly reducing the luminal diameter. (*Photo courtesy of:* University of Wisconsin School of Veterinary Medicine, Department of Pathobiological Sciences, https://www.vetmed.wisc.edu/departments/pathobiological-sciences/)

Microscopic Description:
Esophagus (per submitter): Severely expanding and effacing up to 90% of the submucosa are multifocal to coalescing pyogranulomas composed of a central region of amorphous eosinophilic material (necrosis) admixed with cellular and karyorrhectic debris, surrounded by a ring of intact and fragmented neutrophils, epithelioid macrophages and fewer multinucleated giant cells, and further surrounded by a thin rim of lymphocytes and plasma cells (see Figure 3). Within the central areas of necrosis and rarely within the cytoplasm of multinucleated macrophages are many poorly staining, 7 to 10 µm hyphal organisms with thin non-parallel walls, irregular branching, infrequent septation, and rare bulbous dilations up to 15 µm in diameter (see Figure 4). The hyphal organisms are prominent and exhibit strong dark black staining with a Grocott's Methenamine Silver (GMS) stain (see figure 6) and lack melanin (confirmed with a Fontana Masson's stain). Intersecting between granulomas and further expanding the submucosa are abundant multifocal to coalescing regions of fibrosis and to a much lesser extent hemorrhage, with a few associated macrophages laden with variably sized, golden-brown, intracytoplasmic pigment (hemosiderin). A few granulomas are centered on or extend to adjacent small to medium caliber blood vessels. Affected vessels are often lined by a few necrotic endothelial cells that are occasionally sloughed into the lumen with the tunica intima partially replaced by variable amounts of fibrin and infiltrated by minimal numbers of similar inflammatory cells (fibrinoid necrosis; vasculitis). Within the adventitia, medium to large caliber vessels are frequently surrounded by moderate to large amounts of perivascular fibrosis.

Contributor's Morphologic Diagnosis:
Esophagus: Severe chronic multifocal to coalescing and pyogranulomatous esophagitis with intralesional hyphal organisms

Contributor's Comment:

Given the microscopic features, gross lesions, and morphology of the hyphal organisms, an infection with *Pythium* sp. or *Lagenidium* sp. is considered the cause of disease in this animal despite the results of PCR and sequencing, which identified *Cladosporium* sp. from the formalin fixed tissue. In particular, the microscopic features of this fungus are not consistent with this result and we do not believe that *Cladosporium* species are the source of infection in this animal.

Morphological features consistent with this case and *Pythium/Lagenidium* spp. include non-parallel walls, infrequent septa and irregular branching.[3,5] A few bulbous dilatations within hyphal structures were noted in examined sections which is more consistent with *Cladosporium* sp. as well as the irregular branching and infrequent septa; however, other morphological characteristics of *Cladosporium* sp. include thicker non-parallel walls and apparent pigmentation, which

were not evident.[11] In addition, *Cladosporium* sp. frequently exhibits pigmentation, seen either in routine H&E staining or with the aid of a Fontana Masson's stain, which was not seen in this case. Based on the morphological characteristics, we suspect the hyphal structures are likely *Pythium* sp. or *Lagenidium* sp. regardless of PCR results.

Despite the few morphological similarities shared between *Pythium/Lagenidium* spp. and true fungi, *Pythium* and *Lagenidium* spp. are oomycetes (water molds), not fungal organisms. Key differences between oomycetes and fungal organisms include the lack of chitin within oomycete cell walls and the absence of ergosterol within oomycete cytoplasmic membranes. Additionally, oomycetes undergo sexual reproduction via oogamy.[3]

Oomycetes are typically found in warm stagnant water with *Pythium* sp. having been reported in multiple continents, including North and South America, southern parts of Asia, and Australia. Conversely, *Lagenidium* sp. has only been reported in southern regions of North America.[2-4] Infection with oomycetes are rare in Wisconsin though this dog's recent travel history from Texas was suspect. In dogs, *Pythium insidiosum* and *Lagenidium giganteum* are the most common etiologic agents of pythiosis and lagenidiosis, respectively.[4,13] The life cycle of *Pythium insidiosum* first involves colonization of plants by *Pythium insidiosum* hyphae which then develop into zooporangia, eventually forming zoopores which mechanically break through the vesicle wall and are released into the stagnant water in which the plant resides.[4,8] Zoopores are considered the infective stage and target damaged skin via direct contact or gastrointestinal mucosa if ingested through chemotaxis and its biflagellate motility.[4,8] The zoospores encyst and form hyphal structures similar to the first life stage previously described. Exoantigens cause a T-helper 2 (Th2)-mediated immune response resulting in recruitment of eosinophils which then degranulate resulting in tissue damage.[1,3,4,5,8] With time, the tissue damage will induce more pyogranulomatous inflammation as seen in this case.[3-5] Little is known about the life cycle and pathogenesis of *Lagenidium* sp., though it is likely similar to *Pythium* sp..[4] Some studies have shown that the life cycle and pathogenesis of *Lagenidium* sp. may involve mosquitoes.[13]

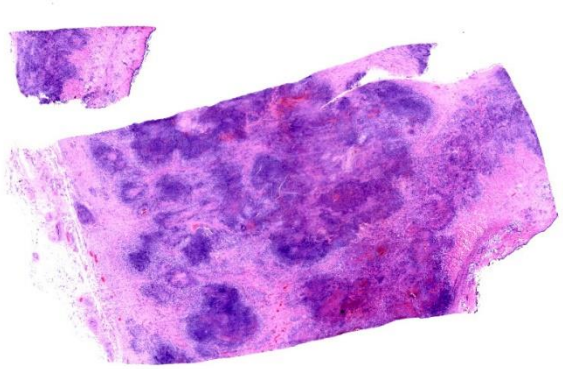

Figure 2-3. Esophagus, dog. Two sections of the esophagus are submitted for examination. The wall is markedly expanded by coalescing areas of inflammation and necrosis. (HE, 4X)

Pythium/Lagenidium sp. have been reported in dogs, cats and humans.[4,11] In addition, *Pythium* sp. have been well-documented in horses and sporadically diagnosed in cattle, sheep, a Californian nestling white-faced ibis, bears, camels, and large cats (i.e. tigers and jaguars).[1,3] In dogs and cats, *Pythium* sp. can cause cutaneous and more frequently, gastrointestinal tract lesions. Infections affecting horses and other documented species are typically limited to the cutis and subcutis.[3,8] In contrast to *Pythium* sp., there are currently no reports documenting gastrointestinal lesions caused by *Lagenidium* sp.. However, *Lagenidium* sp. can cause cutaneous lesions and affect other tissues such as great vessels, sublumbar and inguinal lymph nodes, lung, pulmonary hilus, and cranial mediastinum.[4]

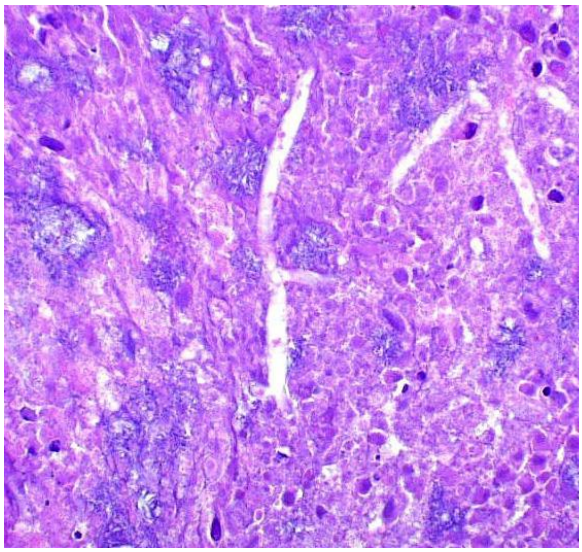

Figure 2-4. Esophagus, dog. Within areas of necrosis, poorly staining hyphal structures exhibit irregular branching and frequently non-parallel walls (HE, 400X) (*Photo courtesy of:* University of Wisconsin School of Veterinary Medicine, Department of Pathobiological Sciences, https://www.vetmed.wisc.edu/departments/pathobiological-sciences/)

When possible, wide surgical excision and various antimicrobial agents and immunotherapeutic drugs have exhibited successful treatment in various species infected with *Pythium*/*Lagenidium* spp.[3,4] Early detection of disease increases the probability of successful treatment; however, in many cases, there fails to be early detection and fatality occurs regularly.[3,4] In addition, local recurrence is common and may occur at the surgical excision site or in a regional lymph node.[4]

Contributing Institution:
University of Wisconsin

School of Veterinary Medicine

Department of Pathobiological Sciences

2015 Linden Drive Madison, WI 53706

https://www.vetmed.wisc.edu/departments/pathobiological-sciences/

JPC Diagnosis:

Esophagus: Esophagitis, necrotizing and pyogranulomatous, chronic-active, multifocal to coalescing, severe, with numerous intrahistiocytic and extracellular hyphae.

JPC Comment:

This second case featured a tricky tissue identification for participants given the marked inflammation, and in this case, features of a somewhat "hidden" organiam were more readily recognized. The nature of the distal esophagus transitioning from a stratified squamous epithelium to columnar epithelium gave some members pause, though this is actually a normal histologic feature[6] and not transitional epithelium (i.e. the urinary bladder).

Dr. Alves emphasized the chronic-active nature of this case. In section, there was a spectrum of inflammatory changes including coalescing areas of necrosis and discrete granulomas as well as maturing granulation tissue and fibrosis. These changes were largely within the serosal tunia, but did expand into the muscularis and submucosa, resulting in degeneration and necrosis of skeletal muscle and loss of esophageal glands in this particular section. GMS and PAS both outlined organisms well in section.

Conference participants then discussed the morphologic findings of the fungal hyphae in this case. We agree with the contributor that the major histologic features of the hyphae are consistent with *Pythium/Lagenidium* sp. and not with *Cladosporium*. Several conference participants raised the possibility of *Conidiobolus/Basidiobolus* sp. as another differential diagnosis. Associated hyphae are typically larger than oomycetes[8] (approximately 5-12 µm and 6-20µm respectively) though have the same irregular branching and rare septations present.[8] Though rare, gastrointestinal basidiobolomyocsis has been rec

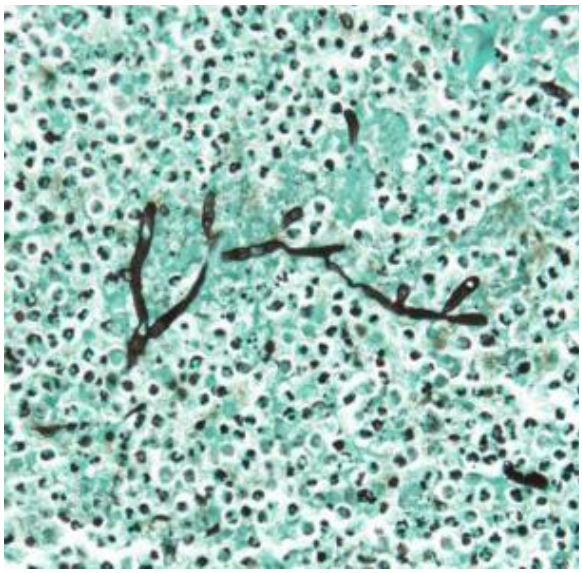

Figure 2-5. Esophagus, dog. Fungal hyphae exhibit strong positivity that highlight the non-parallel walls, infrequent septations and irregular branching (GMS, 200X). (*Photo courtesy of:* University of Wisconsin School of Veterinary Medicine, Department of Pathobiological Sciences, https://www.vetmed.wisc.edu/departments/pathobiological-sciences/)

orded both in the human[11] and veterinary[7] literature. In contrast, *Conidiobolus* is typically associated with respiratory disease in mammals.[7] In histologic section, *Basidiobolus* would be expected to elicit a strong Th2-response similar to what the contributor describes for this case. However, the chronicity of the lesion may also influence whether it is primarily eosinophilic. In this case, the degree of fibrosis and formed granulomas overshadowed eosinophils.

References:

1. Chitasombat MN, Larbcharoensub N, Chindamporn A, Krajaejun T. Clinicopathological features and outcomes of pythiosis. *Int J Infect Dis*. 2018;71:33-41.
2. Chitasombat MN, Jongkhajornpong P, Lekhanont K, Krajaejun T. Recent update in diagnosis and treatment of human pythiosis. *Peer J*. 2020 Feb 20;8:e8555.
3. Gaastra W, Lipman LJ, De Cock AW, Exel TK, Pegge RB, Scheurwater J, Vilela R, Mendoza L. Pythium insidiosum: an overview. *Vet Microbiol*. 2010;146(1-2):1-16.
4. Grooters AM, Pythiosis, lagenidiosis, and zygomycosis in small animals. *Vet Clin Small Anim*. 2003;33:695-720.
5. Grooters AM, Hodgin EC, Bauer RW, Detrisac CJ, Znajda NR, Thomas RC. Clinicopathologic Findings Associated with *Lagenidium* sp. Infection in 6 Dogs: Initial Description of an Emerging Oomycosis. *Vet Intern Med*. 2003;17:637-646.
6. Mann CV, Shorter RG. Structure of the canine esophagus and its sphincters. *Journal of Surgical Research*. 1964 April; 4(4):160-163.
7. Marclay M, Langohr IM, Gaschen FP, et al. Colorectal basidiobolomycosis in a dog. *J Vet Intern Med*. 2020; 34: 2091–2095.
8. Mendoza L, Hernandez F, Ajello L. Life cycle of the human and animal oomycete pathogen Pythium insidiosum. *J Clin Microbiol*. 1993 Nov;31(11):2967-73.
9. Rodrigues Hoffmann A, Ramos MG, Walker RT, Stranahan LW. Hyphae, pseudohyphae, yeasts, spherules, spores, and more: A review on the morphology and pathology of fungal and oomycete infections in the skin of domestic animals. Veterinary Pathology. 2023;60(6):812-828.
10. Romero A, Garcia J, Balestie S, Malfatto F, Vicentino A, Sallis ES, Schild AL, Dutra F. Equine pythiosis in the estern welands of Uruguay. *Pesq Vet Bras*. 2019;39(7):469-475.
11. Velázquez-Jiménez Y, Hernández-Castro R, Romero-Romero L, Salas-Garrido CG, Martínez-Chavarría LC. Feline Phaeohyphomycotic Cerebellitis Caused by *Cladosporium cladosporioides*-complex: Case Report and Review of Literature. *J*

Comp Path. 2019;170:78-85.
12. Vikram HR, Smilack JD, Leighton JA, Crowell MD, De Petris G. Emergence of gastrointestinal basidiobolomycosis in the United States, with a review of world-wide cases. Clin Infect Dis. 2012 Jun;54(12):1685-91.
13. Vilela R, Taylor JW, Walker ED, Mendoza L. *Lagenidium giganteum* Pathogenicity in Mammals. *Emerg Infect Dis*. 2015;21(2):290-297.

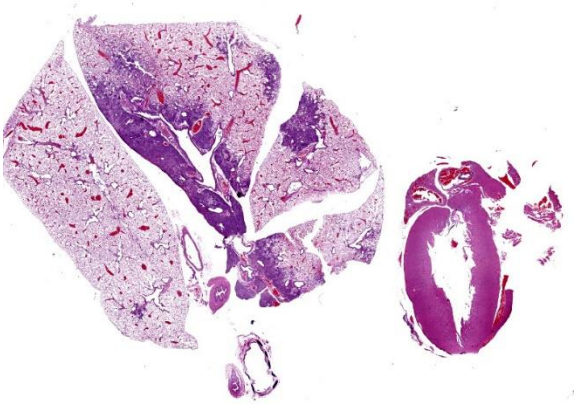

Figure 3-1. Lung, mouse. Approximately 25% of the lung is consolidated by inflammation. A section of heat is submitted as well. (HE, 5X)

CASE III:

Signalment:
6-month-old, female intact, NOD.Cg-*Prkdc*^{scid} *Il2rg*^{tm1Wjl}/SzJ (NSG) mouse (*Mus musculus*). This mouse strain has the *Prkdc* and interleukin 2 receptor *(Il2rg)* mutations, which results in phenotype that lacks numerous immune components including T cells, B cells, natural killer cells, and have deficient signaling for 6 cytokines (IL-2, IL-4, IL-7, IL-9, IL-15, and IL-21). [8]

History:
The mouse was part of experiment in which a NSG mouse shedding *Chlamydia muridarum* was cohoused with four naïve NSG mice. The mouse was lethargic, lost weight, and had a hunched posture and an increased respiratory effort.

Gross Pathology:

The right cranial, middle, and accessory pulmonary lobes were diffusely pale pink to white and atelectatic.

Laboratory Results:
CBC with manual differential showed leukocytosis characterized by mild to moderate neutrophilia and mild monocytosis.

Aerobic and anaerobic cultures of the lung were both negative.

IHC for Chlamydia MOPM-1 showed strong and specific detection of Chlamydia antigen in bronchiolar and alveolar epithelial cells and areas of inflammation.

qPCR for Cm 23S rRNA: Positive in lung

Microscopic Description:
Lung (right and left pulmonary lobes): Affecting approximately 40-45% of the airways in the right pulmonary lobes, there are multifocal to coalescing dense areas of leukocytic cell infiltration mixed with proteinaceous exudate and necrotic cellular debris. Multifocally, alveolar spaces are collapsed and filled with numerous neutrophils and degenerate neutrophils admixed with foamy macrophages, edema, fibrin, karyorrhectic debris and fewer linear clear acicular clefts (cholesterol clefts), and hemorrhage. Alveolar septa are lined by elongated epithelial cells and attenuated necrotic alveolar wall admixed with alveolar macrophages and vacuolated cells containing numerous round basophilic organisms measuring approximately 0.5 to 1.0µm in diameter (Chlamydia elementary and reticular bodies). The adjacent bronchioles are

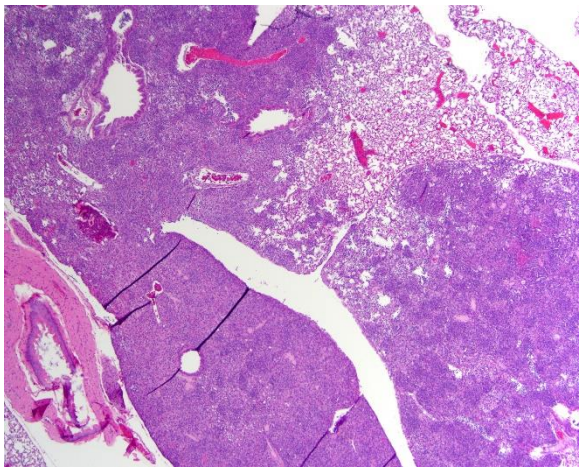

Figure 3-2. Lung, mouse. Areas of pneumonia affect both airways and interstitium (HE, 100X). (*Photo courtesy of*: Laboratory of Comparative Pathology; Memorial Sloan Kettering Cancer Center, Weill Cornell Medicine, Hospital for Special Surgery, and The Rockefeller University https://www.mskcc.org/research/ski/core-facilities/comparative-medicine-pathology-0)

filled by moderate amounts of proteinaceous fluid admixed with neutrophils, karyorrhectic debris, pyknotic cells, and fibrin. The bronchiolar epithelium is segmentally effaced by areas of necrosis and proteinaceous exudate and often contains degenerate bronchiolar epithelial cells with intracytoplasmic vacuoles filled with Chlamydia elementary and reticular bodies (Chlamydia inclusions). Blood vessels are congested and lined by plump endothelial cells with tethered neutrophils. The left pulmonary lobe is multifocally affected by small clusters of neutrophils and foamy macrophages admixed with edema and hemorrhage, predominantly affecting alveoli. Chlamydia inclusions are occasionally noted in the left pulmonary lobe and often observed in the adjacent extrapulmonary bronchi.

Contributor's Morphologic Diagnosis:

Lung: Bronchointerstitial pneumonia histiocytic and neutrophilic, chronic, multifocal to coalescing, moderate to severe, with edema, fibrin, necrotic debris, alveolar histiocytosis, numerous intracytoplasmic Chlamydia inclusions.

Bronchi, tracheal bifurcation: Multifocal intraepithelial Chlamydia inclusions.

Contributor's Comment:

Chlamydia muridarum (Cm) was recently reported as prevalent in research mouse colonies, affecting between 14% and 33% of non-commercial institutions.[5] Cm infections in mice were initially described in the 1930s and 1940s when this bacterium was discovered by accident while inoculating mice with various viruses by transferring lung homogenates.[4,7] In 2021, our group detected Cm inclusions associated with peribronchiolar lymphocytic and plasmocytic aggregates in immunocompetent GEM mouse strains.[4] The case presented in this submission was part of an investigation to evaluate the impact of Cm infection in severely immunocompromised mice (NSG) after cohousing with Cm shedding, naturally infected immunocompetent mice and/or their soiled bedding for 4 weeks.[9] All 19 NSG mice developed pulmonary lesions consistent with bronchointerstitial pneumonia and/or bronchiolitis with numerous intraepithelial Chlamydia inclusions bronchioles and alveoli.[9] Since 2021, our laboratory has reported that Cm infections can be associated with spontaneous clinical disease and pulmonary and/or urogenital pathology in NSG mice and in two genetically engineered mouse (GEM) strains, *Il12rb2* knockout and *STAT1* knockout mice, with impaired interferon-γ signaling and Th1 $CD4^+$ T cell responses.[4,9] As a result of these investigations, testing for Cm has been added to routine health surveillance testing panels in immunocompromised mouse colonies in our institution and commercial breeding colonies in other institutions in the U.S.

Chlamydiae are gram-negative obligate intracellular bacteria with an extensive host range at the genus level, but high host specificity at the species level.[3,7] Cm is the only natural chlamydial pathogen of mice and has been classically used to model the sexually transmitted *Chlamydia trachomatis* infection of humans.[3] Cm exhibits a biphasic life cycle involving a nonreplicating and infectious 'elementary body' and a replicating and noninfectious 'reticulate body.[3,7] Elementary bodies enter the host mucosal epithelial cells and incorporate into a membrane-bound compartment, termed an inclusion body. These elementary bodies then differentiate into reticular bodies. The reticular bodies replicate within the inclusions before reverting into elementary bodies, as which they can then be released and infect nearby cells.[3,7] Natural transmission is via the fecal-oral route, and the gastrointestinal tract is often the natural site of colonization.[14,15] It is thought that pulmonary lesions and colonization can also be acquired through aspiration of inhalation of the organism.[5,9]

The diagnosis of Cm infection in laboratory mice can be confirmed by Cm MOMP-1 IHC and/or qPCR or ISH using Cm-specific primers and probes, respectively.[9] The bronchointerstitial pneumonia and numerous intralesional CI inclusions are characteristic microscopic changes seen in spontaneous and/or experimental Cm infections in NSG mice.[5,9] Cm inclusions are rarely noted in infected lungs from immunocompetent mice[5] and requires the use of ancillary tests for confirmation. Differential diagnoses in immunodeficient mice include bronchopneumonia associated with *Mycoplasma pulmonis* or *Filobacterium rodentium* ("CAR bacillus") and primary viral infections with Sendai virus or Pneumonia Virus of Mice (PVM), granulomatous interstitial pneumonia associated with *Pneumocystis murina*, and bronchopneumonia associated with other opportunistic bacterial agents.[1,10]

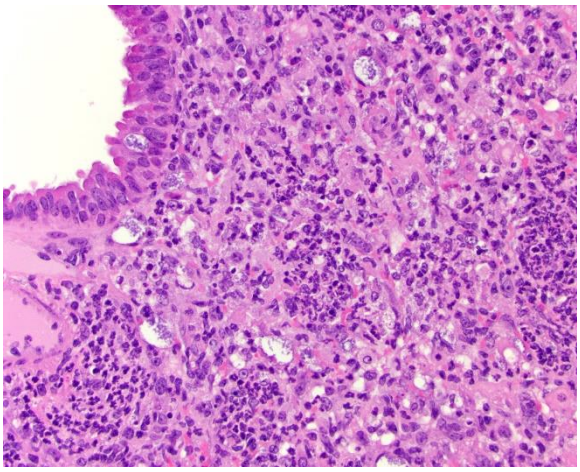

Figure 3-3. Lung, mouse. Peribronchiolar and alveolar spaces are infiltrated by numerous histiocytes and neutrophils admixed with fibrin, edema, karyorrhectic debris, and chlamydial inclusions. (HE, 400X). (*Photo courtesy of*: Laboratory of Comparative Pathology; Memorial Sloan Kettering Cancer Center, Weill Cornell Medicine, Hospital for Special Surgery, and The Rockefeller University https://www.mskcc.org/research/ski/core-facilities/comparative-medicine-pathology-0)

The bronchointerstitial pneumonia and bronchiolitis seen in Cm infected NSG mice shared similarities with pulmonary lesions seen in the acute phase of Cm infection in previous studies using BALB/c and *Tlr2* knockout mice following intranasal challenge.[2,12] Pulmonary lesions in *Il12rb2* knockout and *STAT1* knockout mice naturally infected with Cm are characterized by lymphoplasmacytic and histiocytic inflammation in bronchioles and peribronchiolar and perivascular spaces.[4] Cm inclusions are seen in bronchiolar epithelial cells, but these inclusions are less abundant than the inclusions seen from NSG-infected lungs.[4,9] The severity of the pulmonary lesions seen in NSG mice is likely exacerbated by the absence of CD4+ T and NK cells in this mouse strain.[9] These immune cells are important producers of interferon-gamma (IFN-γ), which is an essential effector cytokine involved in the reso-

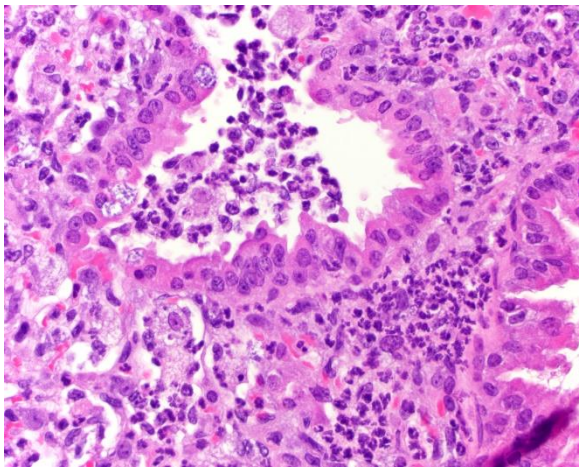

Figure 3-4. Lung, mouse. Histiocytic and neutrophilic bronchointerstitial pneumonia with intracytoplasmic chlamydial inclusions in bronchiolar epithelial cells (HE, 400X). (*Photo courtesy of*: Laboratory of Comparative Pathology; Memorial Sloan Kettering Cancer Center, Weill Cornell Medicine, Hospital for Special Surgery, and The Rockefeller University https://www.mskcc.org/research/ski/core-facilities/comparative-medicine-pathology-0)

lution of Cm infections in experimental models of murine chlamydiosis.[13]

Cm has shown a tropism for mucosal epithelial cells, which serves as a niche for intracellular survival, spread from cell to cell, and immune modulation.[3,6] Cm inclusions in NSG mice were observed in epithelial cells from the nasopharynx, nasal cavity, trachea, eustachian tube, bronchi/bronchioles, oviducts, uterus, and small and large intestines.[9] Among these tissues Cm extensively colonized the small and large intestinal epithelium, without eliciting histopathological changes in the mucosa.[9] Given that NSG mice do not have functional adaptive immune system,[8] Cm likely establishes long-lasting colonization in the intestines and persistent shedding of elementary bodies in feces.

Contributing Institution:
Laboratory of Comparative Pathology; Memorial Sloan Kettering Cancer Center, Weill Cornell Medicine, Hospital for Special Surgery, and The Rockefeller University

417 E. 68th St., ZRC-940

New York, NY 10065

https://www.mskcc.org/research/ski/core-facilities/comparative-medicine-pathology-0

JPC Diagnosis:
Lung: Pneumonia, bronchointerstitial, necrotizing, neutrophilic and histiocytic, subacute, multifocal to coalescing, marked, with numerous intraepithelial bacterial inclusions.

JPC Comment:
This case was recently published in *Veterinary Pathology*[11] and the submitted slides are just as good in person as they are "on paper". The contributor provides a great summary of the paper in their comments, but we invite readers to read it in its entirety in conjunction with this case.

The distribution of *Chlamydia* in this case is generous and the lack of IFN-γ in these mice allowed conference participants to appreciate inclusion bodies readily on H&E, though they stained strongly with PAS as well. Dr. Alves also performed ISH for Chlamydial RNA using a *C. trachomatis* probe which cross-reacted and labeled Cm-infected cells strongly. Additionally, alveolar macrophages (labeled with a F4/80 IHC marker) were assessed, though we did not see actual Chlamydial inclusion bodies within macrophages. Macrophage replication is a feature of *C. trachomatis* infection but was not observed here.

Conference participants also touched on several ancillary changes. In less affected regions of lung, there were numerous alveolar macrophages which was interpreted as alveo-

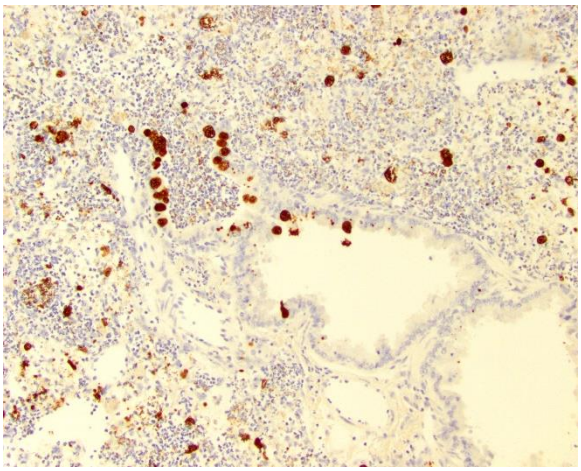

Figure 3-5. Lung, mouse. Chlamydia antigen in inclusions within bronchiolar epithelial cells and scattered in alveolar spaces. Immunohistochemistry (IHC) for Chlamydia major outer membrane protein antigen (MOMP-1). (HE, 400X). (*Photo courtesy of*: Laboratory of Comparative Pathology; Memorial Sloan Kettering Cancer Center, Weill Cornell Medicine, Hospital for Special Surgery, and The Rockefeller University https://www.mskcc.org/research/ski/core-facilities/comparative-medicine-pathology-0)

lar histiocytosis. This is a common background finding in knockout mice. Additionally, the large neutrophilic response in an animal lacking other tools to respond to a pathogen is not surprising – participants noted good examples of leukocyte margination in blood vessels. Though there was also a focus on inflammatory cells along the pericardium, these were interpreted as mast cells as they notably lacked PAS-staining or ISH probe labeling.

There were some indications of chronicity in section. Notably, there is a large, mature thrombus in a pulmonary vein. Additionally, the bronchiolar epithelium is markedly hyperplastic whereas in unaffected sections the epithelium is quite thin. The accumulation of cholesterol crystals is also suggestive of significant loss and accumulation of cell membrane components. In line with the contributor's purported infection timeline[11] we believe that the time course of these changes is at least subacute.

References:

1. Barthold SWP, D.H.; Griffey, S.M. Chapter 1: Mouse In: Barthold SWP, D.H.; Griffey, S.M., ed. *Pathology of Laboratory Rodents*. Fourth ed.: Wiley-Blackwell; 2016:14-81.
2. Beckett EL, Phipps S, Starkey MR, Horvat JC, Beagley KW, Foster PS, Hansbro PM. TLR2, but not TLR4, is required for effective host defence against Chlamydia respiratory tract infection in early life. *PLoS One*. 2012;7**:** e39460.
3. Elwell C, Mirrashidi K, Engel J. Chlamydia cell biology and pathogenesis. *Nat Rev Microbiol*. 2016;14**:** 385-400.
4. Mishkin N, Miranda IC, Carrasco SE, et al. *Chlamydia muridarum* Associated Pulmonary and Urogenital Disease and Pathology in a Colony of Enzootically Infected Il12rb2 Deficient and Stat1 Knockout Mice. *Comp Med*. 2024;74**:** 121-129.
5. Mishkin N, Ricart Arbona RJ, Carrasco SE, et al. Reemergence of the Murine Bacterial Pathogen *Chlamydia muridarum* in Research Mouse Colonies. *Comp Med*. 2022;72**:** 230-242.
6. Perry LL, Hughes S. Chlamydial colonization of multiple mucosae following infection by any mucosal route. *Infect Immun*. 1999;67**:** 3686-3689.
7. Rank RG. Chlamydial diseases. In: Fox JGD, M.T.; Quimby, F.W.; Barthold, S.W.; Newcomer, C.E.; Smith, A.I. , ed. *The mouse in biomedical research*. Burlington (MA): Elsevier; 2007:326-344.
8. Shultz LD, Lyons BL, Burzenski LM, et al. Human lymphoid and myeloid cell development in NOD/LtSz-scid IL2R gamma null mice engrafted with mobilized human hemopoietic stem cells. *J Immunol*. 2005;174**:** 6477-6489.

9. St Jean SC, Ricart Arbona RJ, Mishkin N, et al. *Chlamydia muridarum* infection causes bronchointerstitial pneumonia in NOD.Cg-Prkdc(scid)Il2rg(tm1Wjl)/SzJ (NSG) mice. *Vet Pathol*. 2024;61**:** 145-156.
10. Stair MI, Carrasco SE, Annamalai D, et al. The Epidemiology of Invasive, Multi-pleantibiotic-resistant *Klebsiella pneumoniae* Infection in a Breeding Colony of Immunocompromised NSG Mice. *Comp Med*. 2022;72**:** 220-229.
11. St Jean SC, Ricart Arbona RJ, Mishkin N, et al. Chlamydia muridarum infection causes bronchointerstitial pneumonia in NOD.Cg-PrkdcscidIl2rgtm1Wjl/SzJ (NSG) mice. *Veterinary Pathology*. 2024;61(1):145-156.
12. Virok DP, Raffai T, Kokai D, et al. Indoleamine 2,3-Dioxygenase Activity in *Chlamydia muridarum* and *Chlamydia pneumoniae* Infected Mouse Lung Tissues. *Front Cell Infect Microbiol*. 2019;9**:** 192.
13. Winner H, Friesenhahn A, Wang Y, Stanbury N, Wang J, He C, Zhong G. Regulation of chlamydial colonization by IFNgamma delivered via distinct cells. *Trends Microbiol*. 2023;31**:** 270-279.
14. Yeruva L, Spencer N, Bowlin AK, Wang Y, Rank RG. Chlamydial infection of the gastrointestinal tract: a reservoir for persistent infection. *Pathog Dis*. 2013;68**:** 88-95.
15. Zhong G. Chlamydia overcomes multiple gastrointestinal barriers to achieve long-lasting colonization. *Trends Microbiol*. 2021;29**:** 1004-1012.

CASE IV:

Signalment:
4-year-old, spayed female, Terrier mixed dog (*Canis familiaris*).

Figure 4-1. Myelencephalon, dog. A 0.7 x 0.4 x 0.3 cm, well-demarcated, expansile, white to tan and firm mass effaces the right-side of caudal cerebellar peduncle and the overlying cerebellar cortex. (*Photo courtesy of:* Midwestern University, College of Veterinary Medicine Diagnostic Pathology Center, Glendale, AZ 85308 https://clinics.midwestern.edu/animal-health-institute/diagnostic-pathology-center)

History:
This dog was presented for diarrhea, swollen paw, an increase respiratory, and a brain tumor. The dog had a long history of neurologic signs, facial tremors, ataxia, eye nystagmus, and myotonic like chomping of jaw. TPLO was done in 2023. CT was performed on 02/2024 and revealed a contrast enhancing mass at the right brainstem cerebral region. Valley Fever titers were negative. The patient was on Prednisone, Gabapentin, Diazepam, and Fluconazole. Patient showed continued deterioration including poor ability to open mouth. Euthanasia was elected.

Gross Pathology:
On thoracic examination, there is no pleural effusion. The left lung lobes are pink to dark red and mottle. The lung lobes are soft, aerated, and slightly wet. The distal 1/3 of the trachea and the mainstem bronchi contain a

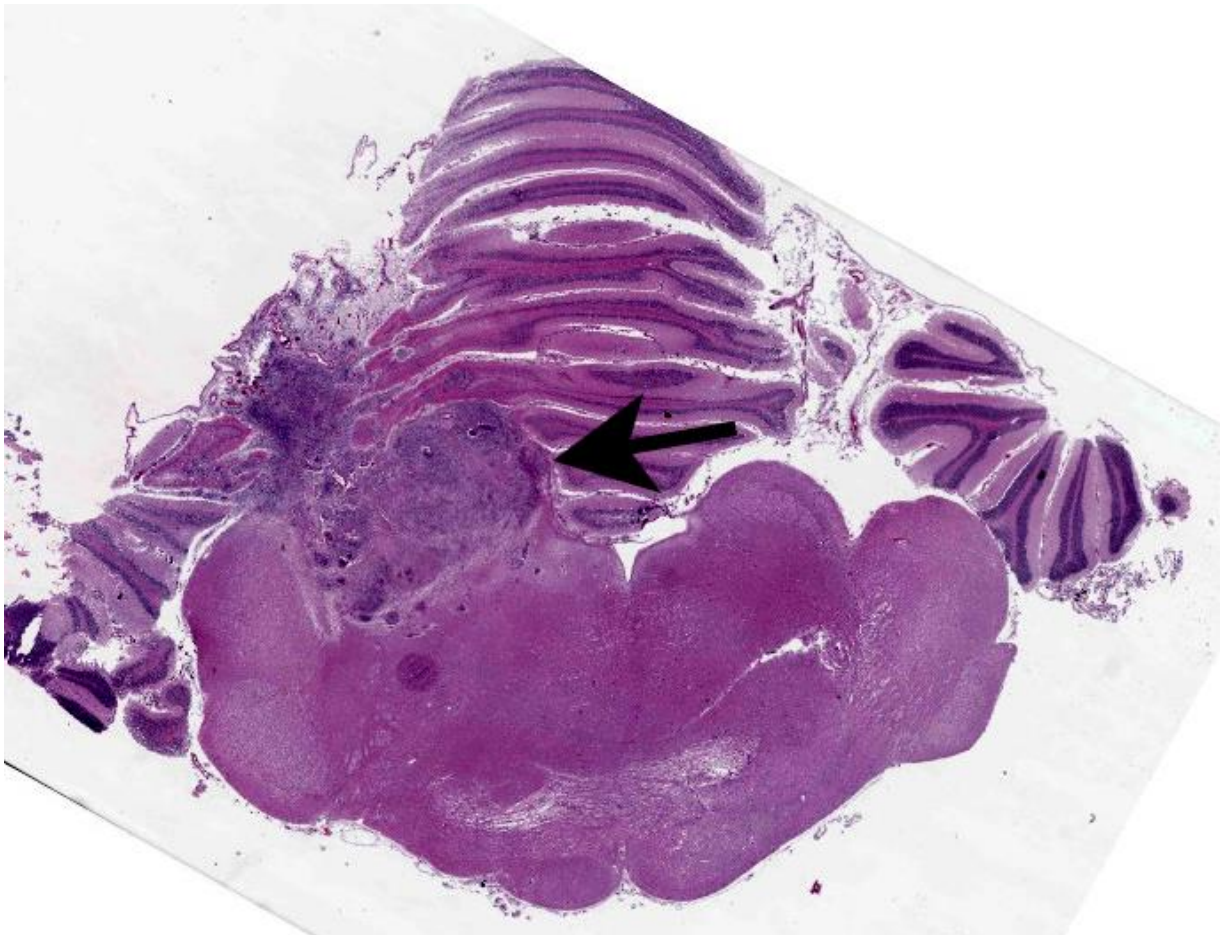

Figure 4-2. Myelencephalon, dog. Subgross magnification of the inflammatory nodule (arrow).

small amount of white froth. There is no pericardial effusion. The heart is unremarkable.

On abdominal examination, the liver is slightly swollen and congested, and weighs 1.36 kg (5% of the patient's body weight). The spleen, pancreas, and GI tract is unremarkable.

On examination of the head and bran, a 0.7 x 0.4 x 0.3 cm, well-demarcated, expansile, white to tan and firm mass effaces the right-side of caudal cerebellar peduncle and the overlying cerebellar cortex.

Clinical pathology:

Two cytospin preparations from the submitted CSF are reviewed. A 90-cell differential

reveals 31 (34%) non-degenerate neutrophils, 52 (58%) small mononuclear cells, 6 (7%) large mononuclear cells, and 1 (1%) eosinophils. The small mononuclear cells are consistent with small to intermediate sized lymphocytes and have occasional single prominent nucleoli. The lightly basophilic protein background contains many erythrocytes and few polychromatophils. No infectious agents or overt evidence of neoplasia is observed.

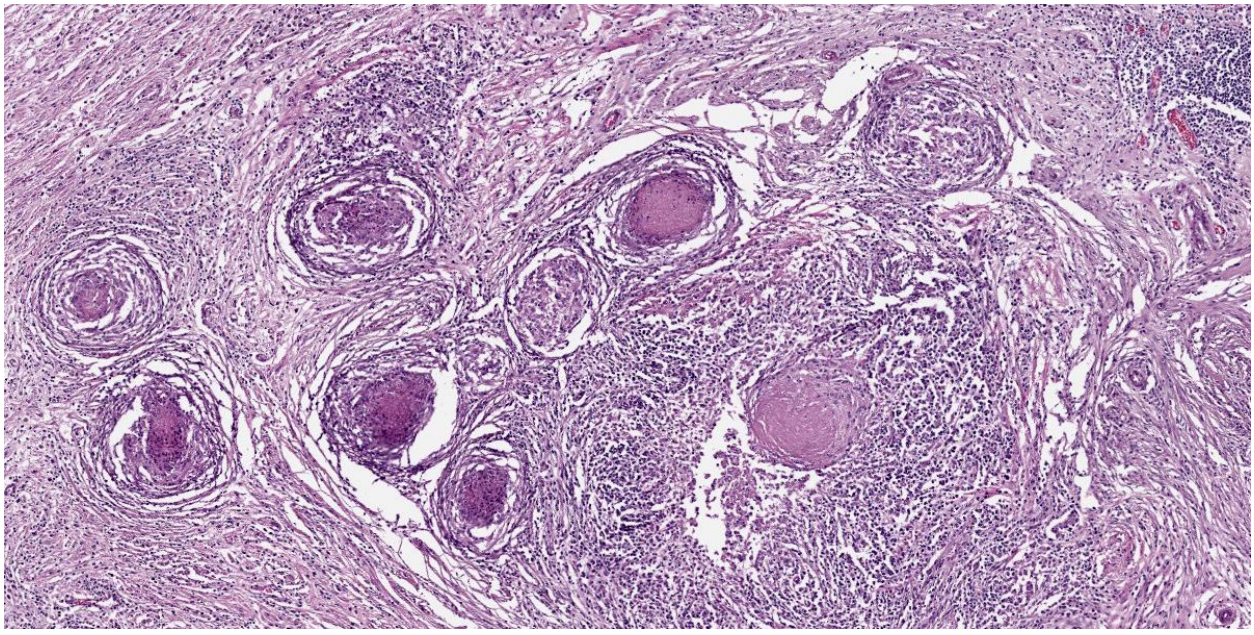

Figure 4-3. Myelencephalon, dog: Numerous granulomas are scattered throughout the inflammatory nodule and surrounding by abundttn fibrous connective tissue extending from the overlying meninges. (*Photo courtesy of:* Midwestern University, College of Veterinary Medicine Diagnostic Pathology Center, Glendale, AZ 85308

and effacing the right caudal cerebellar peduncle, right caudal vestibular nucleus and the overlying cerebellar cortical neuroparenchyma are multifocal to coalescing areas of extensive granulomatous inflammation, characterized by central necrosis and large numbers of epithelioid macrophages, which are surrounded by moderate numbers of lymphocytes, plasma cells, and thin band of fibrous connective tissue. The center of granulomas contain small to large amount of eosinophilic cellular debris, karyorrhectic and pyknotic debris, and degenerate leukocytes that occasionally surround a single, 20-30 um in diameter fungal spherule that has a smooth 4um thick, double contoured, hyaline wall containing multiple granular to flocculent, basophilic structures (endospores), consistent with *Coccidioides* spp. The affected and surrounding neuroparenchyma and meninges to moderate amount of clear space (edema).

Contributor's Morphologic Diagnosis:
Brain, cerebellum and brainstem: Meningoencephalitis, granulomatous, locally extensive, severe, chronic with intralesional fungal spherules (consistent with *Coccidioides* sp.)

Contributor's Comment:
Coccidiomycosis is commonly known as "Valley fever (VF)" and is endemic to human and animals in the southwestern USA (Arizona, California, New Mexico, Nevada) and

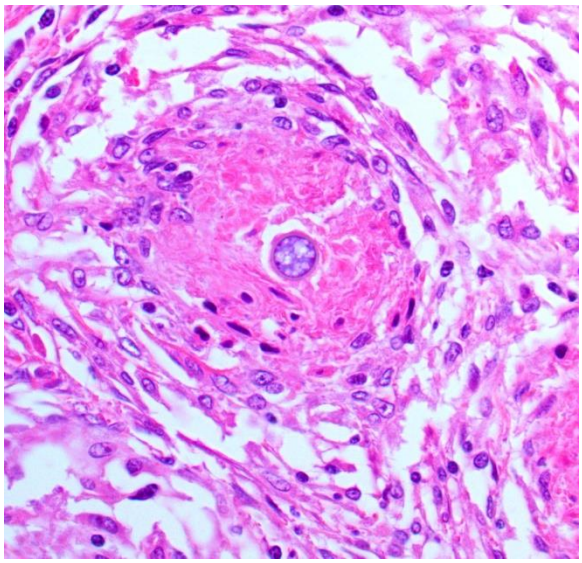

Figure 4-4. Myelencephalon, dog. Granulomas are centered on one or more endosporulating yeasts consistent with *Coccidioides* sp. (*Photo courtesy of:* Midwestern University, College of Veterinary Medicine Diagnostic Pathology Center, Glendale, AZ 85308 https://clinics.midwestern.edu/animal-health-institute/diagnostic-pathology-center)

northern Mexico.[3,7,12] Additional areas are Utah, Eastern Washington, Oregon, Central and South Americas.[14,15] Coccidiomycosis is caused by soil-dwelling, saprophytic, dimorphic fungi, *Coccidioides*. *Coccidioides* was originally described as one species *C. immitis*, but more recently, genetic analysis has defined two separated species with relative distinct geographical distribution. *C. immitis* is largely found in California and Eastern Washington State.[3,15] All cases in Arizona, Texas and Central and South America are *C. posadasii*. There have been no distinct differences in the phenotypical behavior of *C. immitis* and *C. posadasii*.[3,18] *Coccidioides* requires animal nutrients for growth and their distribution which is largely restricted to areas of human or animal habitation, such as small rodent burrows.[3,18] Animal carcasses may serve as a medium for the growth of *Coccidioides* in the soil.[6]

Coccidioides spp. grow in soil as a mycelium. Mycelia septate and produce spores known as arthroconidia which are fragile and become airborne with minimal soil disturbance. The infection is almost always through the inhalation of arthroconidia, rarely cutaneous inoculation, which transform into spherules that subsequently divide into endospores. With spherules lysis, the endospores are released and become spherules which result in exponential propagation in affected organs.[3,6,12]

In humans, 60% of infections are asymptomatic with the remaining 40% having respiratory illnesses. Approximately 1% of total infections are disseminated.[12] In dogs, infection most commonly results in self-limiting respiratory tract disease, but disease can be more severe in some dogs which can result in systemic disease.[14,15] Large breed, young adult dogs are most at risk. Risk factors are increased for outdoor dogs (roaming areas more than 1 acre) and walking in the desert.[4] Boxers, Pointers, Australian Shepherds, Beagles, and Scottish Terriers showed an increased risk of infections as well.[11]

Disseminated coccidioidomycosis includes cutaneous, osseous, cardiac, ocular, and nervous abnormalities along with other signs of systemic illness.[5,9,11] In dogs, CNS involvement typically involves the cerebrum with intracranial lesions often showing focally, or less commonly, as multifocal distinct granulomatous inflammation. Conversely, in human CNS infection, inflammation is more diffuse.[2,13,17] Diffuse, bilateral, symmetric lesions of the caudate nuclei and frontal lobes are less common form in dogs, and the median age of intracranial coccidioidomycosis is 7 years.[13] The time between infections and evidence of disseminated disease ranges from weeks to several years, and a history respiratory signs might not be present.[8,16] Antibody detection is the most sensitive method for VF

diagnosis, but it can be falsely negative in approximately 5-10% of cases.[17] Therefore, coccidioidomycosis should be considered as a potential cause for chronic illness, respiratory signs, lameness, lymphadenopathy, and nonhealing cutaneous lesions, neurological and cardiac illness within endemic regions.

Coccidioidomycosis occurs less frequently in cats, but their presentation and laboratory abnormalities are similar to dogs including respiratory illness, neutrophilia, monocytosis and hyperglobulinemia. However, cats at diagnosis are typically significantly ill and 60% of cats have disseminated infection, most commonly to the skin, in the endemic regions.[1,10]

Contributing Institution:
Midwestern University, College of Veterinary Medicine

Diagnostic Pathology Center

5725 West Utopia Rd.

Glendale, AZ 85308

https://clinics.midwestern.edu/animal-health-institute/diagnostic-pathology-center

JPC Diagnosis:
Cerebellum and brainstem: Meningoencephalitis, granulomatous, chronic, focally extensive, severe, with intra-and extracellular fungal spherules.

JPC Comment:
The contributor provides a nice writeup on coccidiomycosis that prompts some interesting questions for this case. The lesion in this case was focal and unilateral, and extended from the leptomeninges through the cerebellar peduncle and into the brainstem.

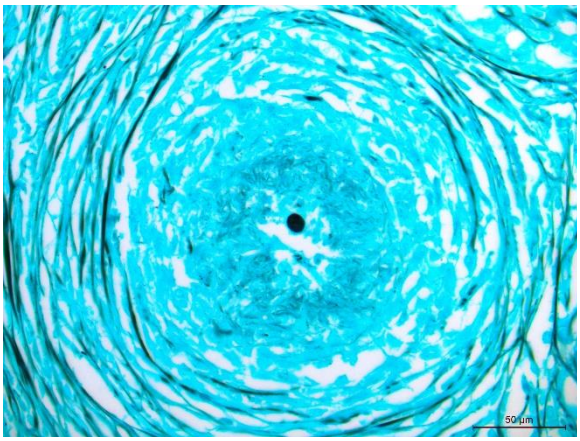

Figure 4-5. Myelencephalon, dog. A silver stain darkly stains the yeast's capsule. (Gomori's methenamine silver, 400X) (*Photo courtesy of:* Midwestern University, College of Veterinary Medicine Diagnostic Pathology Center, Glendale, AZ 85308 https://clinics.midwestern.edu/animal-health-institute/diagnostic-pathology-center)

That this animal reportedly had neurologic deficits attributable to cranial nerve V (motor) and VII deficits aligns with the relative location of these nuclei and the lesion within the brainstem – the focally extensive necrosis of the cerebellum and its role in smoothing motor output likely also played a role, to include the observed nystagmus.

Although the granulomas within the brainstem were an obvious feature on H&E, there were few organisms in histologic section. Even with a GMS or PAS Light Green Stain applied, we noted only 2 granulomas that had an intact spherule. This aligns with the longer clinical course reported by the contributor. Likewise, the lack of free infectious agent (either sequestered in a granuloma and/or low in total number) may have led to a paucity of antigen such that it was below the limit of detection for PCR in this case.

The changes in this case are a classic Th1-response. Participants were quite familiar with Th1 granulomas, though the origin of fibrosis

within the brain was less immediately apparent. With chronic antigen stimulation (such as failing to clear *Coccidioides*), there is predilection for Type-1 macrophages and CD4+ Th1 lymphocytes who in turn produce IFN-γ. IFN-γ is crucial for classical macrophage activation, though this phenotype is notably antifibrotic with cellular arginine being converted to citrulline by nitric oxide synthase 2 which enhances microbicidal activity. In Th2 responses, profibrotic alternatively activated macrophages instead convert arginine to ornithine and eventually proline (a collagen precursor). While the normal brain parenchyma lacks fibroblasts to create fibrous tissue, there are two potential sources to strategically acquire them. In this case, the extension of inflammation through to the meninges (and associated meningeal fibroblasts) is the most likely explanation. Alternatively, differentiation of perivascular fibroblasts (from pericytes) is another possibility that may explain some of the fibrosis deeper in tissue section.[7] The disruption of the blood-CNS barrier may also play a role.[7]

References:

1. Arbona N, Butkiewicz CD, Keyes M, et al. Clinical features of cats diagnosed with coccidioidomycosis in Arizona, 2004-2018. *J Feline Med Surg*. 2020 22(2):129-137.
2. Bentley RT, Heng HG, Thompson C, et al. Magnetic resonance imaging features and outcome for solitary central nervous system Coccidioides granulomas I 11 dogs and cats. *Vet Radiol Ultrasound*. 2015 56(5):520-530.
3. Brown J, Benedict K, Park BJ, et al. Coccidioidomycosis: epidemiology. *Clin Epidemiol*. 2013 25(5):185-197.
4. Butkiewicz CD, Shubitz LF, Dial SM. Risk factors associated with Coccidioides infection in dogs. *J Am Vet Med Assoc*. 2005;226(11):1851-1854.
5. Davidson AP, Shubitz AF, Alcott CJ, et al. Selected Clinical Features of Coccidioidomycosis in Dogs, *Medical Mycology*, 2019, S67–S75.
6. Del Rocio Reyes-Montes M, Ameyali Perez-Huitron M, Luis Ocana-Monroy J, et al. The habitat of *Coccidioides* spp. and the role of animals as reservoirs and disseminators in nature. *BMC Infectious Diseases*. 2016;16:550.
7. Fehlberg CR, Lee JK. Fibrosis in the central nervous system: from the meninges to the vasculature. Cell Tissue Res. 2022 Mar;387(3):351-360.
8. Galgiani JN, Ampel NM, Blair JE, et al. Infectious Diseases Society of America (IDSA) Clinical Practice Guideline for the Treatment of Coccidioidomycosis. *Clin Infect Dis*. 2016 15;63(6):e112-146.
9. Graupmann-Kuzma A, Valentine BA, Shubitz LF, et al. Coccidioidomycosis in dogs and cats: a review. *J Am Vet Med Assoc*. 2008;44(5):226-235.
10. Greene RT, Troy GC. Coccidioidomycosis in 48 cats: a retrospective study (1984-1993). *J Vet Intern Med*. 1995, 9(2):86-91.
11. Johnson LR, et al., Clinical, clinicopathologic, and radiographic findings in dogs with coccidioidomycosis: 24 cases (1995-2000). *J Am Vet Med Assoc*, 2003. 222(4):461-466.
12. Johnson RH, Sharma R, Kuran R, et al. Coccidioidomycosis: a review. *J Investig Med*. 2021, 69(2):316-323.
13. Kelley AJ, Stainback LB, Knowles KE, et al. Clinical characteristics, magnetic resonance imaging features, treatment, and outcome for presumed intracranial coccidioidomycosis in 45 dogs (2009-2019). *J Vet Intern Med*. 2021, 35(5):2222-2231.
14. Lockhart SR, McCotter OZ, Chiller TM. Emerging Fungal Infections in the Pacific Northwest: The Unrecognized Burden and Geographic Range of *Cryptococcus gattii* and *Coccidioides immitis*. *Microbiol Spectr*. 2016. 4(3).
15. Meisner J, Clifford WR, Wohrle RD, et al.

Soil and climactic predictors of canine coccidioidomycosis seroprevalence in Washington State: An ecological cross-sectional study. *Transbound Emerg Dis*. 2019. 66(5):2134-2142.
16. Shubitz LF, Butkiewicz CD, Dial SM, et al. Incidence of Coccidioides infection among dogs residing in a region in which the organism is endemic. *J Am Vet Med Assoc*. 2005;226(11):1846-1850.
17. Spoor E, Stainback L, Plummer S, et al. A novel form of intracranial coccidioidomycosis is present in dogs and exhibits characteristic clinical and magnetic resonance imaging findings. *Vet Radiol Ultrasound*. 2019. 60(1):47-55.
18. Taylor JW, Barker BM. The endozoan, small mammal reservoir hypothesis and the life cycle of Coccidioides species. *Med Mycol*. 2019, 1(57):S16-S20.